Investigation of the Air Flow in a generic Model of the Lung:
Analysis of the Governing Transport Mechanisms

Lars Krenkel

Institute of Aerodynamics and Flow Technology, Dept. Fluid Systems
German Aerospace Center (DLR)
Bunsenstr.10, 37073 Göttingen, Germany
Lars.Krenkel@dlr.de

Claus Wagner

Institute of Aerodynamics and Flow Technology, Dept. Fluid Systems
German Aerospace Center (DLR)
Bunsenstr.10, 37073 Göttingen, Germany
Claus.Wagner@dlr.de

ABSTRACT

The central airways of the lung are a complex system of bifurcations and pipes. In the case of artificial ventilation support with the necessity of using airway management devices (i.e. endotracheal tubes) the complexity of the system even increases and a complete understanding of the ventilation and oxygenation mechanisms is of major interest in order to ensure protective oxygenation and ventilation of the patient.

Numerical investigations on the influence of endotracheal tubes on the flow revealed that thesel tubes have an important impact within the trachea and accordingly in the central airways of the lung. A parametric study on the effect of the tube's level of detail on the resulting flow regime showed that it is necessary to model not only the tube's ending but also the bending which is essential for the development of secondary flows.

A comparison of numerical data generated with a turbulent and a laminar Navier-Stokes solver revealed that for the indistinct, potentially transitional flow in the airways with endotracheal tube the simulations with turbulence model are more promising but in terms of computational costs more expensive.

INTRODUCTION

Since a large number of patients admitted to the intensive care unit require artificial ventilation support the development of lung protective ventilation strategies is an important subject in biomedical research. The central airways of the lung are a complex system of bifurcations and pipes with characteristic diameters ranging from approx. 15 mm to 20 mm at the trachea to approx. 50 μm to 250 μm at alveolar level. The lungs principle task to ensure the gas exchange is intimately depending on the fluid mechanical transport mechanisms governing the complex branching system. For patients suffering from adult respiratory distress syndrome (ARDS), acute lung injury or at the worst from acute lung failure, mechanical ventilation is the fundamental life saving therapy but even after years of practical experience and research the mortality rate is still high. This is related to inspiratory lung epithelia overstretching and repeated collapse and re-expansion of alveoli which results in adverse shear forces which in turn tend to aggravate the aetiopathology finally leading to ventilator associated lung injury (VALI).

In case of artificial ventilation support with the necessity of using airway management devices (i.e. endotracheal tubes) the complexity of the system even increases and a complete understanding of the ventilation and oxygenation mechanisms is of major interest in order to ensure protective oxygenation and ventilation of the patient.

Protective Artificial Ventilation

The objective of the protective artificial lung ventilation strategy is to achieve an improved gas exchange in the lungs while applying ventilation methods which allow for avoidance of inspiratory epithelial overstretching and repeated collapse and re-expansion of alveoli. A promising lung protective ventilation approach is the "High Frequency Ventilation Oscillation (HFOV)". The HFOV concept was introduced in the early 1960s as a new ventilation technique for treating the neonatal respiratory distress syndrome (RDS). Today it is also used as a rescue therapy for patients with acute respiratory distress syndrome.

A proper understanding of the fluid mechanical mechanisms governing the HFOV is essential for optimising this artificial ventilation approach in terms of protective, efficient, and reliable oxygenation and ventilation of patients suffering from acute respiratory failure.
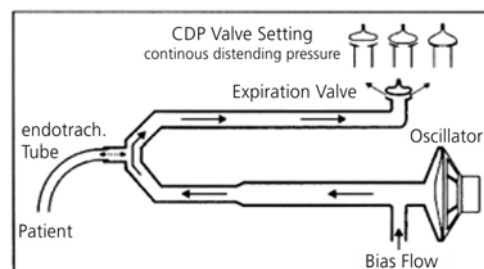
Figure 1: Functional principle of HFOV [ViasysHC]

The concept of lung protective ventilation strategies is based on the limitation of the inspiratory pressure and the reduction of the tidal volume, in order to minimize the extent of breathing cycle-dependent damaging mechanisms thus minimising the presence of high intra-alveolar shear forces. These undesired shear forces are contributing to a great extent to the ventilation associated lung injury (VALI).

NUMERICAL STUDY OF ENDOTRACHEAL TUBE FLOWS

According to Haberthür et al. [Haberthür2009] and Guttmann et al. [Guttmann1995], in tracheally intubated and mechanically ventilated patients, expiratory resistance of an endotracheal tube or a tracheostomy can cause dynamic lung hyperinflation by impending lung emptying. Furthermore, analysing experimental data from animal HFO ventilation experiments and results from experiments in the magnetic resonance tomograph at the University of Mainz [Schreiber2009] focusing on the governing flow field in a generic trachea with endotracheal tube as well as from other research groups ([Rocco1995], [Menon1986], [Gavriely1985]) it became apparent that the flow in the endotracheal tube strongly affects the flow field in the lung. Another important factor is that due to different length scales in the airways including the airway management devices (tube, connector, etc.), the Reynolds number varies from below 1000 in the upper central airways to 4000 or even higher in the endotracheal tube. Even if the flow may be assumed to be laminar almost everywhere in the central airways, it is expected to be turbulent within and in the vicinity of the endotracheal tube.

Analysis of experimental artificial ventilation data with respect to typical velocity fields and characteristic Reynolds numbers revealed that in most cases turbulent regions with Reynolds numbers exceeding 2300 are expected only in or in the vicinity of the endotracheal tube and the first few bifurcations at very high inspiratory or expiratory flow rates. For higher branch generations and at lower flow rates the flow regime is supposed to be laminar. From a theoretical point of view it seems to be straight forward that an accurate prediction of the turbulent flow is only possible with either Direct Numerical Simulations (DNS) and Large Eddy Simulations (LES) or Reynolds-averaged Navier-Stokes (RANS) simulations with a properly chosen turbulence model as well as an optimized mesh geometry. Thus, the question arises, whether a RANS solver provides accurate simulation results for the mostly laminar flow regime regions apart from the most likely turbulent endotracheal tube flow.

Numerical Methods and Tools

For the numerical simulations the DLR in-house Code THETA was used. The descretised volume mesh was generated with the hybrid commercial grid generator package CENTAUR™. A description of the numerical tools will be given in the following subsections.

The DLR THETA Code. The DLR finite volume code THETA solves the incompressible Reynolds-averaged Navier-Stokes equations on unstructured grids. For steady simulations the SIMPLE method and for unsteady time resolved simulations the Projection method is used for the pressure-velocity coupling. The discretisation of the momentum and other transport equations is based on the quadratic upstream difference scheme (QUDS). For additional convergence acceleration, a V3 multi grid cycle was applied for solving the Poisson equation together with a least square gradient reconstruction algorithm. Furthermore, the domain decomposition approach was used for efficient parallel computing. In terms of turbulence modelling the THETA code allows either to use a standard (low Reynolds number) k-ω turbulence model with near wall resolution or with additional application of general wall functions or a standard (high Reynolds number) k-ε model together with wall functions. For this study, two turbulence models, the low Reynolds number k-ω model (wall resolved without and in a second step with generalised wall functions), and the high Reynolds number k-ε model with wall functions were used in addition to simulations without turbulence modelling.

Numerical Mesh Generation. The commercial software package CENTAUR™ was used for volume mesh generation of the different geometrical set-ups. Figure 2 shows a typical highly resolved hybrid mesh of a tube with Murphy's eye placed in a generic trachea.
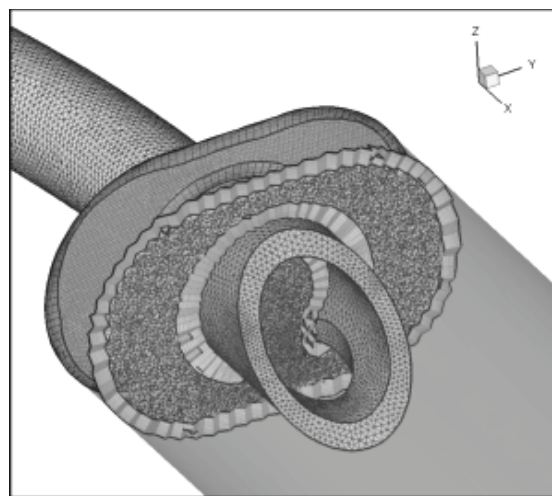
Figure 2: Illustration of the surface and volume mesh resolution at the endotracheal tube

The picture shows the surface mesh of the tube and the abstracted tube's cuff as well as a cut plane through the volume mesh. A typical hybrid mesh used for the investigations consist of approx. 3.5 mio nodes with a pseudo structured prism sub-layer (10 prism layers) for better resolution of the boundary layer close to the wall and an unstructured tetrahedral part. With increasing distance downstream of the tube's ending, the mesh was coarsened in order to reduce the amount of grid points.

At first, a study with different mesh resolutions had been carried out in order to ensure grid independency of the solutions. Afterwards all meshes were generated with identical mesh generator settings to achieve to some degree similar meshes in terms of resolution.
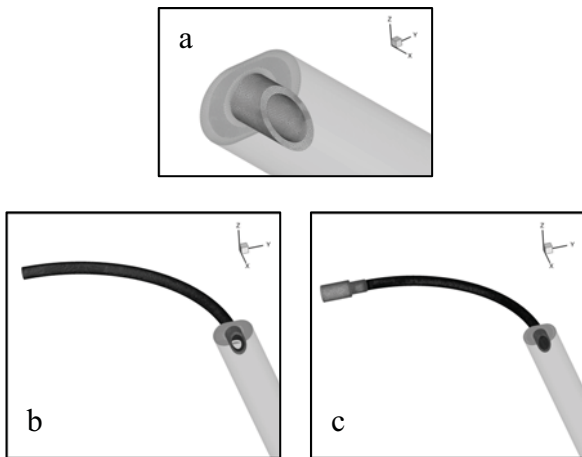
Figure 3: Selection of investigated geometries:
a) straight tube ending   b) tube with bending and
Murphy eye   c) tube with bending and connector

Variation of the Tube Model Geometry

Numerical simulations were carried out focusing on the impact of the tube model geometry, with respect to their level of detail, on the resulting flow field. A set of 6 different geometries was investigated numerically using the DLR THETA code. The following results were obtained using a standard low Reynolds number k-ω turbulence model for unsteady, time resolved parallel RANS simulation (time step: 0.005 sec, CFL<1) of each case. The bulk inlet velocity for each case was set to match a Reynolds number of 1500 based on the average velocity in

the generic trachea resulting in a maximal Reynolds number based on the tube diameter and the average velocity in the tube of approx. 3300. The generic trachea has a length of 1.5 m and the tracheal profile consists of two semi-circles (Ø20 mm) which are pulled apart 10 mm in one direction (characteristic lengths: height 20 mm, width 30 mm). In total 6 different set-ups were investigated. One set-up consisted of a generic trachea with abstracted endotracheal tube. The level of detail of the tube was changed stepwise beginning with a very simple model of a straight tube's ending, going over a 35 cm long tube with 90 degrees bending, and ending up with a highly detailed tube with bending and connector. All three geometries were also tested with an additional so-called Murphy eye, a small hole at the tube's tip. Figure 3 depicts the three base geometries, but figure 3b represents exemplary the geometry with an additional Murphy eye close to the tube's outlet.

The predicted results for the three geometries without Murphy eye are presented in figure 4. The upper picture of each case shows the distribution of turbulent kinetic energy. The lower picture reflects the iso-surface of the swirl $s = (U \cdot \omega) / (\rho \cdot \|U\|)$ for a constant value of "s=-300" (U: local velocity, ω: vorticity, ρ: density). It is obvious that the simple straight tube ending does not show any secondary flow structures in contrast to the bended tubes. The iso-surface of swirl can be interpreted as a visualisation of the three-dimensionality of the flow. The higher the value or the higher the amount of iso-surfaces the stronger the helical/rotational motions (velocity vector parallel to vorticity vector) of the flow. A Comparison of the two cases with bending reveals only slight differences in swirl and turbulent kinetic energy distribution but reflects, as expected, with higher level of turbulent kinetic energy
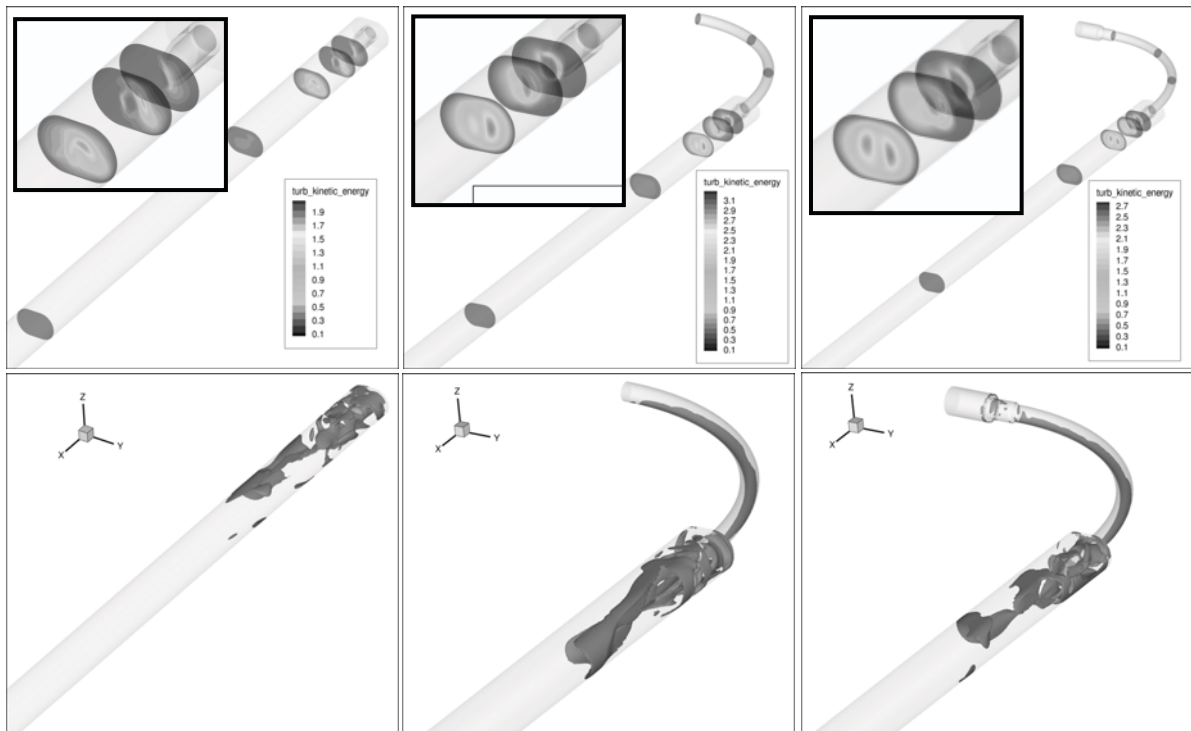
Figure 4: Comparison of CFD data: distribution of turbulent kinetic energy (upper row)
and iso surface visualisation of swirl (lower row)

compared to the simple tube ending case. A more detailed comparison of turbulent kinetic energy (k) distribution reveals clearly the effect of the bending which induces secondary flow structures and, in this particular case, two secondary velocity rolls. For the case with connector, the absolute level of turbulent kinetic energy is slightly lower than for the case without connector but the secondary flow structures seem to be more pronounced (two clearly shaped regions, of higher turbulent kinetic energy instead of one high level spot and one blurred region).

Considering the swirl plots, the connector seems to enhance the formation of secondary velocity rolls and furthermore to enhance the mixing of the flow downstream of the tube outlet. This results in a regionally reduced swirl iso-surface extension for the case with connector in comparison to the case without connector. Figure 5 and Figure 6 show a comparison of the predicted horizontal and vertical velocity profiles taken at 4 different positions downstream of the tube's ending for the two cases with and without connector.
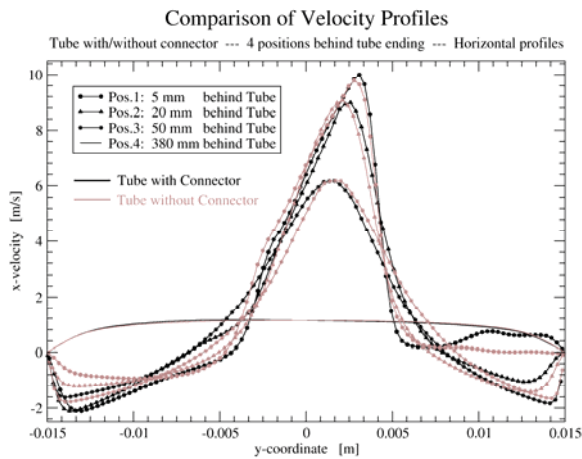
Figure 5: Comparison of computed velocity profiles at 4 positions downstream of the tube (horizontal cuts)
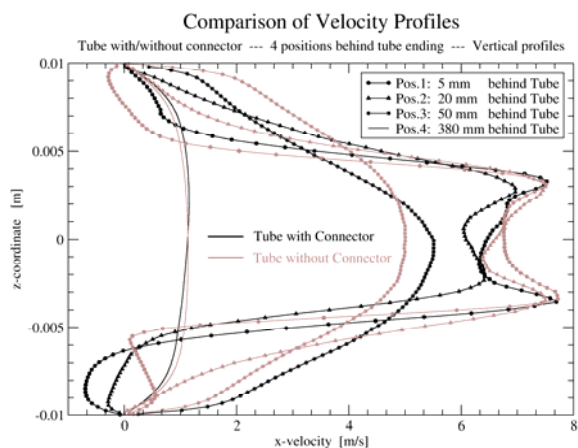
Figure 6: Comparison of computed velocity profiles at 4 positions downstream of the tube (vertical cuts)

Especially the vertical velocity profiles reveal the effect
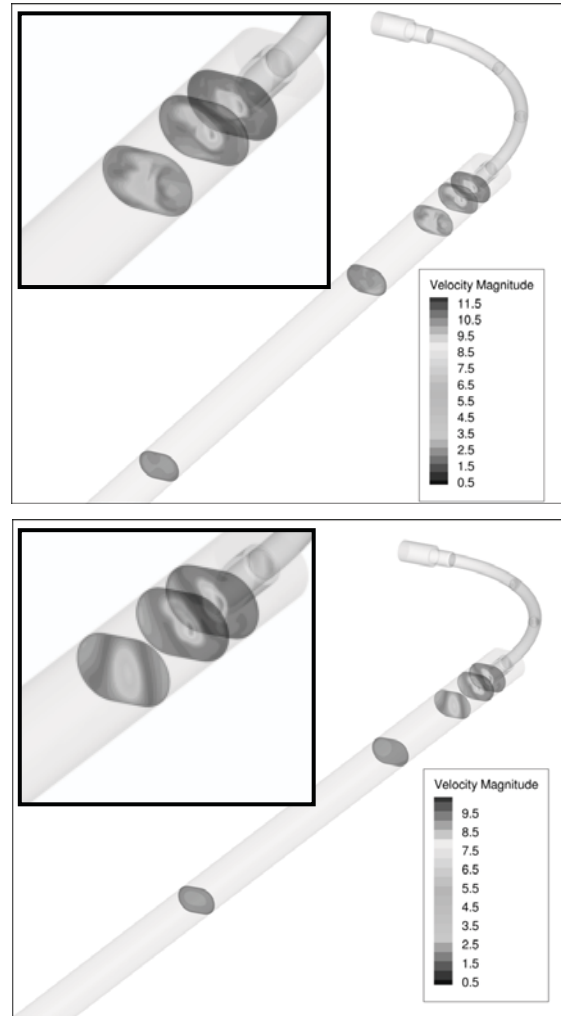
Figure 7: Comparison of results obtained with (turbulent – lower) and without (laminar – upper) turbulence model

of the connector on the flow field. The set-up with connector tends to lead to more asymmetric profiles which might be interpreted as an indication for the development of more pronounced secondary flow structures and enhanced cross mixing. To a certain extend, the profiles are similar in terms of curve characteristics and magnitude but show differences especially close to the generic trachea's limiting wall and in the vicinity of the tube's outlet. This is most likely related to the generation of vortical structures and mixing at the discontinuous change in cross section area in the connector.

A comparison of cases with and without Murphy eye hardly showed any significant differences. The strongest effect can be observed in the vicinity of the eye where a local re-circulation area develops which slightly affects the jet formation at the main outlet of the tube. Therefore, it is concluded that a detailed modelling of the tube geometry is essential for obtaining sufficient resolved flow predictions for these cases. Using a strongly abstracted simple tube ending instead of a complete tube model yields incorrect

results due to disregarding important secondary flow structures. On the other hand are details like Murphy eyes negligible since there impact on the resulting flow field is rather low.

Impact of Turbulence Modelling on the Flow Field

Even for physiological ventilation gases, the Reynolds number exceeds the critical value of 2300 within the endotracheal tube which indicates that there might be turbulent flow regions. It is also well known from measurements that a turbulent flow can develop in the upper part of the central airways (first to fourth bifurcation) at very high inspiratory and expiratory flow rates and for small diameters of the endotracheal airway management devices (e.g. tubes, connectors, etc.). For higher branch generations and at lower flow rates the flow is expected to be and to stay laminar. From a theoretical point of view it seems to be clear that an accurate prediction of the turbulent flow is only possible with a properly chosen turbulence model. Therefore the question arises, whether the Navier-Stokes solver also provides accurate predictions for regions where the flow is laminar.

Figure 7 depicts a line-up of laminar and turbulent flow simulations in terms of velocity distributions downstream of the tube. At the outlet of the tube the laminar and the turbulent results are similar but the homogenisation and the settling of the flow appears to happen much faster if a turbulence model is used.

This is most probably due to the stronger turbulent mixing which is enhanced by the turbulence model in terms of additionally introduced turbulent dissipation. Based on the numerical data it seems appropriate to perform simulations together with modelling even if the turbulent flow regions are limited to the tube and the vicinity of the outlet. The production rate of turbulent kinetic energy in regions with expected laminar character is negligible. It seems that due to the introduced turbulent dissipation the general dissipative

terms are slightly overestimated. This leads to a higher level of damping which has to be verified in further comparison with additional experimental data.

COMPARISON OF EXPERIMENTAL AND NUMERICAL DATA

Figure 8 shows a comparison of experimental magnetic resonance (MR) based velocity measurements in a generic trachea with 9 mm tube and RANS simulations for a similar geometry. The bulk inlet velocity was adjusted for a mean tracheal Reynolds number based on the mean velocity of 1500, resulting in a maximal Reynolds number of 3300 in the endotracheal tube. The only geometrical difference of both set-ups can be found in the rather simplified modelling of the tube, i.e. only the straight ending and not the complete 90° bending of the tube has been shaped. In general, both results agree well. The laminar velocity profile is well reproduced in the experimental data but with a difference in the peak velocity at the centre line. The observed difference is most likely related to a too coarse resolution of the experimental data (voxel size approx. 2 mm x 2 mm x 2 mm), and to the fact that the velocity encoding MR technique has sometimes problems with the signal to noise ratio at low flow velocities. In some cases this leads to flattened velocity profiles as it is observed in this particular case.

Although the flow is supposed to be laminar and the velocity gradient close to the wall indicates a laminar velocity profile the peak velocity is cut. This gives the impression of a not fully developed laminar flow. Further experimental investigations on this specific topic are under way.

Furthermore, there is a small but noticeable deviation with respect to velocity profile (slightly stronger curvature into positive y direction). This might be a result of the simplified representation of the tube which prevents the development of secondary flow structures as induced by the
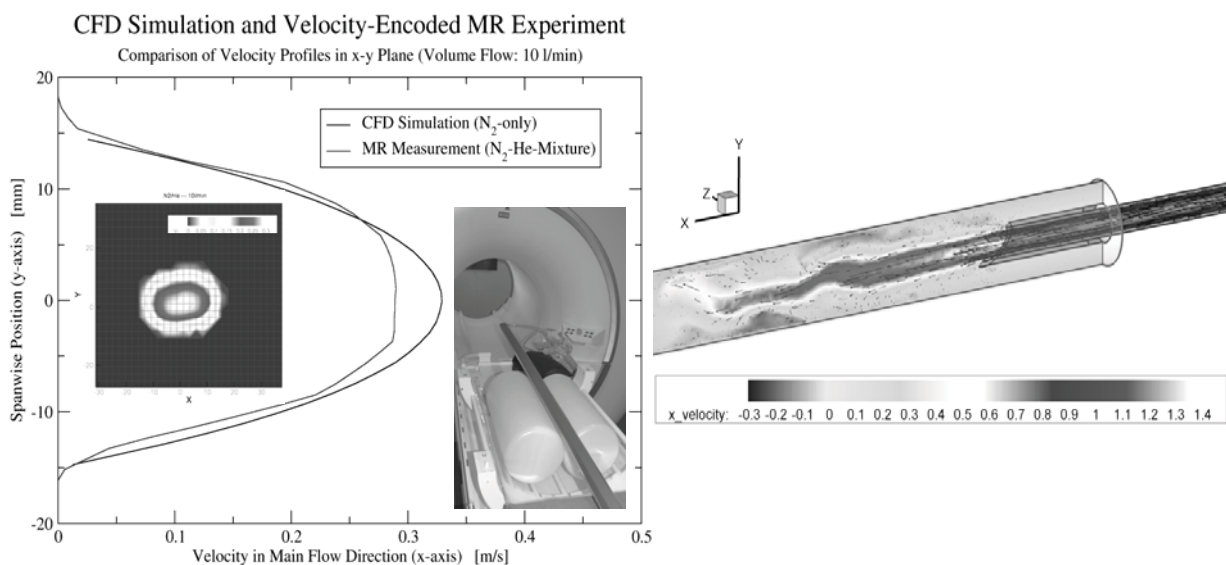
Figure 8: Comparison of numerical and experimental data of the flow in a generic trachea
with 9 mm endotracheal tube (Gas: Helium)

Sixth International Symposium on Turbulence and Shear Flow Phenomena
Seoul, Korea, 22-24 June 2009

normal 90° tube bending. This agrees well with the consolidated findings of the impact of tube model geometry on the resulting flow field in a generic trachea.

FUTURE WORK

In order to gain better knowledge on the complex transport mechanism in the lung it is necessary to investigate more complex geometries and to apply more realistic boundary conditions. With high resolution meshes of the central airway reconstructed from medical image data and newly implemented total pressure open boundary conditions, which allow for simulation a complete artificial ventilation cycle (inspiration and expiration), it will be possible to simulate even complex flow phenomena in the upper central airways, taking into account pathological conditions (e.g. acute respiratory distress syndrome - ARDS). Figure 9 illustrates a more complex mesh of a 4th generation lung with endotracheal tube.
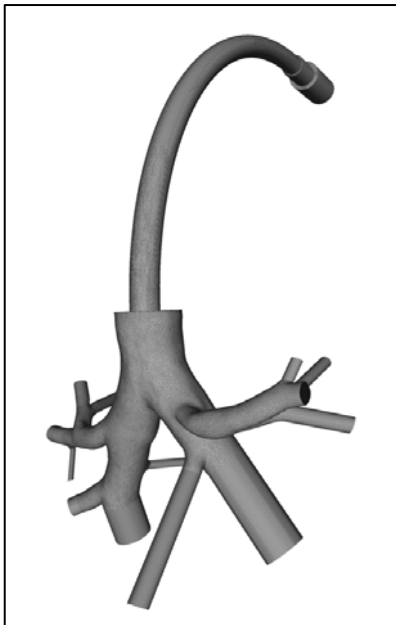
Figure 9: Geometry for investigation of tube impact
on the flow regime of more complex geometries

CONCLUSION

Numerical investigations of the impact of endotracheal tubes on the flow revealed that endotracheal tubes have an important impact within the trachea and accordingly in the central airways of the lung. A numerical parametric study on the effect of the tube's level of detail on the resulting flow regime showed that it is necessary to model not only the tube's ending but also the bending which is essential for the development of secondary flows. A symmetrical flow regime 20 diameters downstream of the tube was found with a fully resolved tube with bending whereas the tube with bending and connector generates stronger vortical structures resulting in a slightly asymmetric velocity field. A final validation with further experimental data and further analysis of the influence of the turbulence models as well as mesh resolution studies in comparison to Direct Numerical Simulations are under way.

A comparison of numerical data generated with a turbulent and a laminar Navier-Stokes solver revealed that for the indistinct, potentially transitional flow in the airways with endotracheal tube the simulations with turbulence model are more promising but in terms of computational costs more expensive. Validation with detailed experimental data will be accomplished soon. Further numerical and experimental investigations focusing on more complex configurations using a 4th generation cast model are in preparation.

REFERENCES

Gavriely, N., Solway, J., Loring, S.H., et al., 1985, "Pressure-flow relationships of endotracheal tubes during high-frequency ventilation", *J ApplPhysiol*, Vol 59, pp. 3-11.

Guttmann, J., Eberhard, L., Fabry, L., 1995, "Time constant/volume relationship of passive expiration in mechanically ventilated ARDS patients", *Eur Respir J*, Vol.8, pp. 114-120.

Haberthür, C., Mehlig, A., Stover, J.F. et al., 2009, "Expiratory endotracheal tube compensation reduces dynamic hyperinflation in a physical lung model", *Critical Care*, Vol.13, No.1.

Menon, A.S., Weber, M.E., and Chang, H.K., 1986, "Velocity profiles in central airways with endotracheal intubation: a model study", *J Appl Physiol*, Vol. 60, pp. 876-884.

Rocco, P.R.M., and Zin, W.A., 1995, "Modelling the mechanical effect of tracheal tubes in normal subjects", *Eur Respir J*, Vol. 8, pp. 121-126.

Schreiber, L.M. et al., 2009, "Private Communications", University Mainz.